



Cite this: *Phys. Chem. Chem. Phys.*,  
2024, 26, 21040

# Enhancing protein stability under stress: osmolyte-based deep eutectic solvents as a biocompatible and robust stabilizing medium for lysozyme under heat and cold shock†

Anja Damjanović,<sup>‡a</sup> Marijan Logarušić,<sup>‡a</sup> Lidija-Marija Tumir,<sup>‡b</sup>  
Thanos Andreou,<sup>‡c</sup> Marina Cvjetko Bubalo,<sup>‡\*a</sup> and Ivana Radojčić Redovniković<sup>a</sup>

In biomedical and biotechnological domains, liquid protein formulations are vital tools, offering versatility across various fields. However, maintaining protein stability in a liquid form presents challenges due to environmental factors, driving research to refine formulations for broader applications. In our recent study, we investigated the relationship between deep eutectic solvents (DESs) and the natural presence of osmolytes in specific combinations, showcasing the effectiveness of a bioinspired osmolyte-based DES in stabilizing a model protein. Recognizing the need for a more nuanced understanding of osmolyte-based DES stabilization capabilities under different storage conditions, here we broadened the scope of our osmolyte-based DES experimental screening, and delved deeper into structural changes in the enzyme under these conditions. We subjected lysozyme solutions in DESs based on various kosmotropic osmolytes (TMAO, betaine, sarcosine, DMSP, ectoine, GPC, proline, sorbitol and taurine) paired either with another kosmotropic (glycerol) or with chaotropic osmolyte urea to rigorous conditions: heat shock (at 80 °C) and repetitive freeze–thaw cycles (at –20 and –80 °C). Changes in enzyme activity, colloidal stability, and conformational alterations were then monitored using bioassays, aggregation tests, and spectroscopic techniques (FT-IR and CD). Our results demonstrate the remarkable effectiveness of osmolyte-based DES in stabilizing lysozyme under stress conditions, with sarcosine- and betaine-based DESs containing glycerol as a hydrogen bond donor showing the highest efficacy, even at high enzyme loadings up to 200 mg ml<sup>-1</sup>. Investigation of the individual and combined effects of the DES components on enzyme stability confirmed the synergistic behavior of the kosmotrope–urea mixtures and the cumulative effects in kosmotrope–glycerol mixtures. Additionally, we have shown that the interplay between the enzyme's active and stable (but inactive) states is highly influenced by the water content in DESs. Finally, toxicity assessments of osmolyte-based DESs using cell lines (Caco-2, HaCaT, and HeLa) revealed no risks to human health.

Received 4th June 2024,  
Accepted 12th July 2024

DOI: 10.1039/d4cp02275k

rsc.li/pccp

## Introduction

Within biomedical and biotechnological domains, liquid protein formulations have emerged as invaluable tools due to their inherent versatility and practical advantages. They play pivotal roles across diverse fields, spanning from the development of biopharmaceuticals and protein-based drugs to biotechnological processes like enzyme production, diagnostic assays,

and biocatalysis, which all rely on stable proteins throughout all stages of manufacturing (expression, purification, and formulation), shelf-life management, and product administration/application.<sup>1–4</sup> One notable characteristic of liquid protein formulations is their capacity to ensure superior sample homogeneity, as proteins in solution are uniformly distributed, thus guaranteeing consistent sample quality. Additionally, the liquid form facilitates seamless mixing, dilution, and aliquoting of proteins, eliminating the need for cumbersome reconstitution steps and enhancing operational efficiency.<sup>2</sup>

However, for proteins in a liquid form, the delicate balance of their structure can be easily disrupted by environmental factors such as changes in temperature and pH, as well as mechanical stress. These disruptions often lead to denaturation, inactivation, and aggregation of proteins, resulting in a

<sup>a</sup> Faculty of Food Technology and Biotechnology, University of Zagreb, Croatia.

E-mail: mcvjetko@pbf.hr

<sup>b</sup> Ruđer Bošković Institute, Zagreb, Croatia

<sup>c</sup> VIO Chemicals AG, Thessaloniki, Greece

† Electronic supplementary information (ESI) available. See DOI: <https://doi.org/10.1039/d4cp02275k>

‡ These authors contributed equally to this work.



loss of functionality and product quality.<sup>5,6</sup> To evaluate protein formulation stability, heat- and freezing-induced protein denaturation has emerged as rapid and reliable methods. These processes disrupt the native structure of proteins when exposed to extreme temperatures, allowing researchers to quickly observe changes in protein stability and gain insights into potential degradation pathways. Additionally, this type of denaturation simulates conditions that proteins may encounter during storage or processing, enhancing its relevance for evaluating formulation stability.<sup>1,7,8</sup>

To aid in the folding or refolding of proteins in liquid protein formulations, especially under stressful conditions, chemical chaperones are frequently used.<sup>9,10</sup> Naturally occurring osmolytes, including methylamines, sugars, alcohols, and amino acids, have been demonstrated as excellent chaperones of proteins in numerous cases.<sup>11</sup> When incorporated into formulations, these molecules mimic their natural role *in vivo*, which is to protect biological systems (such as extremophilic bacteria, marine organisms, sporulating microorganisms, and plants) from stressful environmental conditions by providing thermodynamic stability to biomacromolecules, particularly proteins, without compromising their natural functionality.<sup>12</sup> Another relatively new class of chemical chaperones that also effectively mimic the natural environment of biomolecules to stabilize them are non-toxic and highly versatile systems known as deep eutectic solvents (DESs).<sup>13,14</sup> Originally, the term DES was coined to describe a physical mixture of two or more components, usually from natural sources, that solidifies at a single temperature lower than the crystallization point of any individual component.<sup>15</sup> With time, these solvents/systems have evolved to include mixtures of two or more components that demonstrate properties similar to a eutectic system,<sup>16</sup> with one fixed criterion: remaining in a liquid state at a specified temperature, even if one of its components would normally be solid and unsuitable for use as a solvent.<sup>17</sup> The chaperon-like activity of DESs for various proteins, such as lysozyme,<sup>18–20</sup> lipases,<sup>21,22</sup> collagen peptide,<sup>23</sup>  $\alpha$ -chymotrypsin,<sup>24</sup> laccases,<sup>25,26</sup> bovine serum albumin,<sup>27</sup> various peroxidases,<sup>28</sup> cellulases,<sup>29</sup> human interferon,<sup>30</sup>  $\beta$ -galactosidase,<sup>31</sup> immunoglobulin G,<sup>32</sup> and ubiquitin,<sup>33</sup> has been reported so far.

In our recent study,<sup>34</sup> for the first time, a connection was established between two previously parallel approaches to protein stabilization: osmolytes- and DES-assisted protein stabilization. Intrigued by the structural similarity between osmolytes and common DES components, as well as the fact that osmolytes are typically present in cells and tissues in certain combinations and molar ratios, we investigated a set of natural osmolytes and patterns of their natural distribution, preparing new bioinspired two-, three-, and multi-component DESs based on osmolytes. The newly prepared bioinspired solvents were further assessed as a protein stabilization medium at room temperature. The results indicate superior stabilization compared to conventional DESs and the standard buffer used for protein storage. Building upon that research, in this study we subjected lysozyme solution in various DESs to rigorous conditions, including heat shock at 80 °C and multiple

freeze–thaw cycles at –20 °C and –80 °C. The stabilizing effect of DESs was examined using bioassays and spectroscopic methods. Finally, as osmolytes accumulate in times of stress, the results are discussed within the framework of osmolyte-based presence *in vivo*, suggesting a universal mechanism of action used by living systems during periods of stress.

## Experimental part

### Materials

Lysozyme extracted from hen egg white and *Micrococcus lysodeikticus* (ATCC No. 4698) was purchased from Sigma-Aldrich (St. Louis, MI, USA). All components of the DESs were also procured from Sigma-Aldrich. All chemicals were of at least 99% purity and were used without additional purification.

### DES preparation and characterization

DESs were prepared in the way that two or more components in specific ratios with a certain amount of water (20, 40, 60 or 80% of water (w/w)) were placed in a glass flask, stirred, and heated at 50 °C until a clear homogeneous liquid was formed (Table 1).

Upon cooling to room temperature, the mixture was left on a bench for a week to observe possible solidification or precipitation. Before use, DES forming compounds choline chloride, TMAO and sarcosine were dried in a vacuum drier (Memmert GmbH + Co. KG) at 40 °C and 100 mbar for 24 h. The pH of all DESs was measured at room temperature using a pH electrode (InLab<sup>®</sup> Micro Pro-ISM pH electrode, Mettler-Toledo). The density at room temperature was measured by using a pycnometer ( $V = 1$  ml). To determine the polarity and molar transition energy (ENR) of the DESs Nile red was used as a solvatochromatic probe.<sup>35</sup>

### Extent of lysozyme aggregation

Heat-induced aggregation of lysozyme solution (5 mg ml<sup>–1</sup>) in DESs and the referent solvent (50 mM potassium phosphate buffer, pH 6.4) was studied using a temperature-controlled UV/vis spectrophotometer (Lambda 35, PerkinElmer). A sample was placed in a quartz cuvette and covered with mineral oil to retard evaporation. Turbidity changes ( $\lambda = 600$  nm) were monitored at a temperature of 80 °C.

### Lysozyme activity assay

Lysozyme activity was determined according to the method of Shugar *et al.*<sup>36</sup> Briefly, 30  $\mu$ l of *Micrococcus lysodeikticus* bacteria suspension in sterile PBS buffer (7 mg ml<sup>–1</sup>) and 30  $\mu$ l of the lysozyme solution were added to 525  $\mu$ l of 50 mM potassium phosphate buffer solution (pH 6.4) in a cuvette. Immediately after mixing, the cuvette was placed in a UV/vis spectrophotometer (Thermo Fisher Scientific, GenesysTM10S) and the absorbance was measured at a wavelength of 450 nm over a period of linear turbidity decline. Relative activity was calculated as a ratio of activity measured in the DES and the activity measured in the reference buffer.



**Table 1** Physicochemical properties and cytotoxicity of DESs used for lysozyme stability screening. The water content for all used DESs was 40% (w/w)

DES	Abbreviations <sup>a</sup>	Molar ratio	pH (20 °C)	$E_{NR}$ [kcal mol <sup>-1</sup> ]	$\rho$ (20 °C) [g cm <sup>-3</sup> ]	$EC_{50}$ (mg ml <sup>-1</sup> )		
						HaCaT	Caco-2	HeLa
Choline-based DES	ChCl:U	1:2	7.7	48.98	1.13	ND	ND	ND
	ChCl:Gly	1:2	6.2	49.60	1.14	ND	ND	ND
Betaine-based DES	Bet:U	1:1	8.1	49.96	1.14	ND	ND	ND
	Bet:Gly	1:2	6.0	49.72	1.15	ND	ND	ND
Sarcosine-based DES	Sar:U	2:5	5.6	49.75	1.19	> 1000	> 1000	> 1000
	Sar:Gly	1:2	5.2	49.48	0.88	> 1000	> 1000	> 1000
Ectoine-based DES	Ect:U	1:2	6.8	48.92	1.20	> 1000	> 1000	> 1000
	Ect:Gly	1:2	6.3	49.78	1.15	> 1000	> 1000	> 1000
TMAO-based DES	TMAO:U	1:1	9.6	49.79	1.09	> 1000	> 1000	> 1000
	TMAO:Gly	1:2	9.1	50.43	1.14	> 1000	> 1000	> 1000
Proline-based DES	Pro:U	1:2	7.2	49.81	1.16	> 1000	> 1000	> 1000
	Pro:Gly	1:2	6.2	49.93	1.18	> 1000	> 1000	> 1000
DMSP-based DES	DMSP:U	1:2	5.6	48.67	1.19	> 1000	> 1000	> 1000
	DMSP:Gly	1:2	1.0	48.54	1.18	310.2	335.5	380.9
Bioinspired	Bet:U:Gly:U	1:3.1:0.1:2.8:7.1	7.0	49.24	1.18	> 1000	> 1000	> 1000
multicomponent DES	TMAO:Bet:Tau:U	1:6:0.5:15	6.8	49.34	1.16	> 1000	> 1000	> 1000

<sup>a</sup> Choline–chloride (ChCl), betaine (Bet), sarcosine (Sar), ectoine (Ect), trimethylamine N-oxide (TMAO), proline (Pro), dimethylsulfoniopropionate (DMSP), urea (U), glycerol (Gly), sorbitol (Sor), taurine (Tau), glycerophosphocholine (GPC).

### Residual activity of lysozyme after heat shock and freeze–thaw conditions

Lysozyme solutions at a concentration of 5 mg ml<sup>-1</sup> (0.1 mg ml<sup>-1</sup> for preliminary screening on the influence of the water content on DES ability to stabilize lysozyme; 50, 100 and 200 mg ml<sup>-1</sup> for experiments related to the stability of highly concentrated lysozyme solutions) were prepared in different DES and in 50 mM potassium phosphate buffer solution (pH 6.4). Enzyme solutions were subjected to different storage conditions: (i) incubation for 1 hour at 80 °C; and (ii) freeze–thaw conditions: 24-hour freeze–thaw cycle at –20 °C or –80 °C, total of 5 cycles.

Residual lysozyme activity after each storage condition was determined according to the method of Shugar *et al.*<sup>36</sup> described above. In brief, an aliquot of lysozyme solution in DES was withdrawn, and the residual activity was measured. The residual activity (%) was calculated from the initial reaction rate obtained by the enzyme after incubation, compared to the one obtained without previous exposure.

### Circular dichroism (CD) measurements

CD spectra of lysozyme dissolved in 50 mM potassium phosphate buffer solution (pH 6.4) or relevant DESs (final protein concentration of 0.2–0.75 mg ml<sup>-1</sup>) were recorded on a JASCO J815 spectrophotometer (Jasco Corp., Tokyo, Japan), with a Peltier cell holder for temperature control.

CD spectra in the near UV region (250–350 nm) were obtained at a fixed temperature (20 °C, 80 °C or 95 °C) with a scan rate of 200 nm min<sup>-1</sup>, a bandwidth of 1 nm and a response time of 1 s. Near UV CD spectra were recorded using appropriate 1 cm path quartz cuvettes, except for Ect:Gly solution (path of 0.5 cm). Concentrations of lysozyme were 0.75 mg ml<sup>-1</sup> (52 μM). Each spectrum was accumulated for 2 scans. Baselines taken with DES or buffer under the same conditions were subtracted from each spectrum.

CD spectra in the far UV region (190–250 nm) were measured at room temperature in the wavelength range of 200–250 nm with a scan rate of 200 nm min<sup>-1</sup>, bandwidth of 1 nm and a response time of 1 s. Due to the high absorbance of DES,<sup>37,38</sup> far UV CD spectra were recorded using appropriate 0.1 mm path quartz glasses to avoid HT voltage above 600 V. The concentration of lysozyme was 0.2 mg ml<sup>-1</sup> (15 μM). The study of far-UV spectra of lysozyme after storage in the DES was performed by hydration:<sup>39</sup> diluting of DES with buffer, to achieve a final DES content of 0.5% (w/w). The spectra after hydration were recorded using 1 cm path quartz cuvettes.

Thermal CD-scans were collected at a fixed wavelength (227 ± 5 nm) in a temperature range 20 °C to 95 °C in appropriate 1 mm path quartz cuvettes at a heating rate of 1 °C per minute. The concentration of lysozyme was 0.3–0.4 mg ml<sup>-1</sup> (20–26 μM). Ellipticities ([θ]) were expressed in observed mdeg and in units of deg cm<sup>2</sup> dmol<sup>-1</sup>, using the protein concentration.

### Fourier transform infrared spectroscopy (FT-IR)

FT-IR spectra of the mixtures, spectra of the pure starting compounds, and spectra of lysozyme solutions in DESs (20 mg ml<sup>-1</sup>) and 50 mM potassium phosphate buffer solution (pH 6.4) were recorded on an FT-IR spectrometer equipped with an attenuated total reflection module (Tensor II, Bruker, Ettlingen, Germany) with diamond ATR crystal from 4000–400 cm<sup>-1</sup>, with a resolution of 4 cm<sup>-1</sup>. The spectra are the average of 16 scans. For measurements of protein solutions (20 mg ml<sup>-1</sup>), the samples were left to equilibrate for 1 h prior to measurements, with all measurements being made in the next 1 h. FT-IR spectra of each solvent, without the protein present, were acquired under the same conditions and used for solvent subtraction.

### Cytotoxicity assay

The cytotoxicity of DESs was tested against three human adherent cell lines: cancer cells derived from the colorectal adenocarcinoma



(Caco-2 – ATCC No. HTB-37<sup>TM</sup>), normal human keratinocyte cells (HaCaT – CVCL No. 0038), and epithelial cells from cervical carcinoma (HeLa – ATCC No. CCL-2<sup>TM</sup>). Cells were maintained in DMEM – Dulbecco's modified Eagle's medium (Capricorn Scientific GmbH), supplemented with 5% (v/v) FBS – fetal bovine serum (GIBCO by Life Technologies) in an incubator with 5% CO<sub>2</sub> and a humidified atmosphere at 37 °C. The impact of synthesized DESs on cellular proliferation was investigated *in vitro* utilizing the CellTiter96<sup>®</sup> Aqueous One Solution Cell Proliferation assay (Promega), also known as the MTS assay. Briefly, cells were seeded in 96-well plates at a density of  $3 \times 10^4$  cells per well in 100  $\mu$ l of media. Following overnight incubation, cells were exposed to the prepared DESs at three concentrations spanning from 100 to 500, and ultimately 1000 mg ml<sup>-1</sup>, and then incubated for 72 hours. A 10  $\mu$ l volume of MTS reagent was added to each well and the absorbance was measured at 492 nm on the microplate reader after the 3-hour incubation period. Cell viability percentage was calculated by comparing the absorbance of treated cells to that of untreated control cells. The experiments were conducted in triplicate with four replicates for each concentration. The corresponding EC<sub>50</sub> values, defined as the concentration of tested compounds leading to 50% growth inhibition, were calculated from the dose–response curves.

## Results and discussion

In our previous work, we showcased the ability of novel osmolyte-based DESs based on kosmotropes sarcosine, ectoine and DMSP (all HBAs), when paired with glycerol as a HBD, to stabilize a model protein (lysozyme) at 25 °C to a greater extent than the conventional choline chloride-based DES (ChCl:Gly) and the reference buffer.<sup>34</sup> This was also confirmed for bioinspired multicomponent DES replicated from an osmolyte cocktail in mammalian kidneys comprising chaotrope urea. To gain a deeper understanding of novel osmolyte-based DESs' capacity

to stabilize lysozyme, this study expanded both the range of DESs utilized and the incubation conditions applied to enzyme solutions in DESs. Lysozyme was once again chosen for its cost-effectiveness, the accessibility of rapid and reliable spectrophotometric methods for activity measurement, and the wealth of information available on its behaviour under various conditions *in vitro*.<sup>40</sup> In this research, we first prepared and characterized various osmolyte-based DESs in terms of their physicochemical properties and cytotoxicity (Table 1). Following this, lysozyme solutions in DESs were subjected to stressful conditions, including heat shock or repeated freezing–thawing cycles (Fig. 1), whereby the stabilizing effect of DESs was examined using bioassays and spectroscopic methods.

### Osmolyte-based DESs preparation and characterization

Versatile DESs were prepared for analysis by combining a range of components, such as kosmotropic osmolytes (trimethylamine-*N*-oxide (TMAO), betaine, sarcosine, dimethylsulfiniopropionate (DMSP), ectoine, glycerophosphocholine (GPC), proline, glycerol, sorbitol, and taurine) and chaotrope urea (Table 1). It is important to note that the osmolytes utilized in this study span across all kingdoms of life, ranging from deep-sea fish (TMAO, sarcosine, and urea), plants (betaine), fungi (ectoine and glycerol), algae (DMSP), to mammals (GPC and urea). DESs based on choline chloride and the osmolyte betaine, which have already been established as effective lysozyme stabilizers<sup>41–44</sup> were prepared and tested as well.

Preliminary experiments investigating the impact of water content on the solvent's ability to stabilize lysozyme at 80 °C, conducted on a limited selection of DESs (ChCl:Gly, Sar:Gly and Ect:Gly), revealed that lysozyme was either more effectively or equally stabilized in DESs containing 40% water (w/w) compared to those with 20% water (with a difference of  $\pm 10\%$ ; data not shown). A water content of 40% was also considered beneficial from a practical standpoint: water helps reduce the

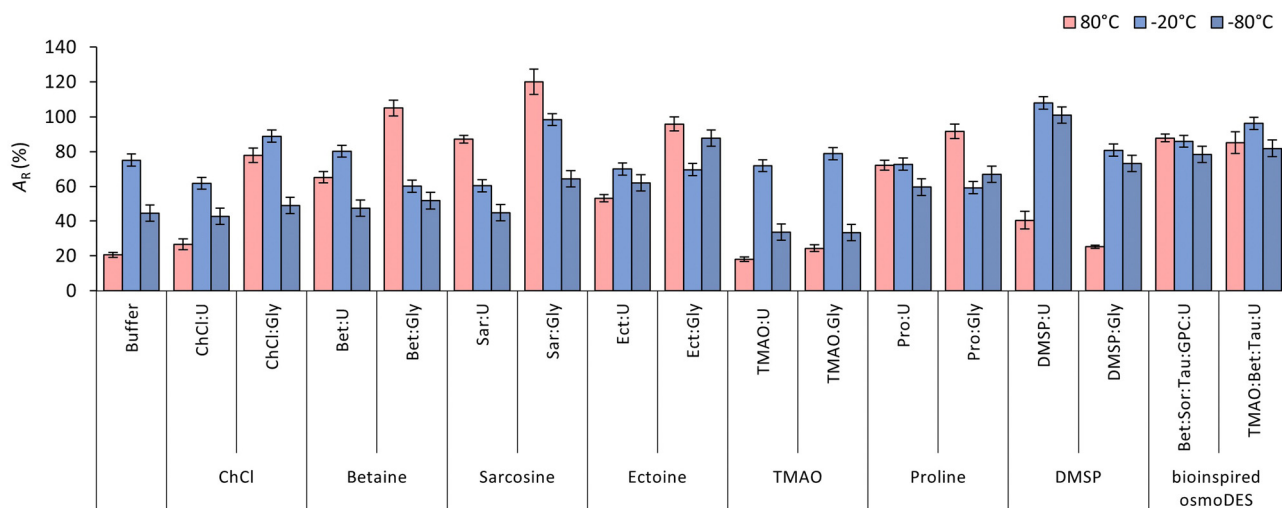


Fig. 1 Residual lysozyme activity ( $A_R$ ) after incubation in DESs (40% of water, w/w) and 50 mM potassium phosphate buffer solution (pH 6.4) after: heat shock (1 hour at 80 °C) or five freeze/thaw cycles at  $-20$  °C and  $-80$  °C ( $c_{Lys} = 5$  mg ml<sup>-1</sup>). The residual lysozyme activity ( $A_R$ ) was calculated from the initial reaction rate obtained by the enzyme after incubation, compared to the one obtained without previous exposure.



solvent's viscosity<sup>45</sup> making it easier to handle and potentially suitable for larger-scale applications.<sup>46</sup> At this point, dilutions of DESs beyond 40% were not considered, as additional water would result in a solvent behaving more like a solution of its components in water.<sup>47</sup>

In accordance with the above, a total of fourteen two-component osmolyte-based DESs and two bioinspired multi-component DESs, all containing 40% water (w/w), were prepared and characterized (Table 1). The pH value of the prepared DESs ranged widely: from 1.0 (DMSP:Gly) to 9.8 (TMAO:U). In general, the most acidic DESs were those with DMSP (pH 1.0 and 5.6) and sarcosine (pH 5.2 and 5.6) as HBA, while TMAO-based DESs were shown to be basic (pH 9.1 and 9.6). This is not surprising, as it is well-established that the acidity/basicity of a DES originates from its starting components, which in this case significantly differ from one another (e.g., the  $pK_a$  values of sarcosine, ectoine, TMAO, glycerol, and urea are 2.2, 3.1, 7.7, 13.5, and 13.9 respectively). Furthermore, DMSP was utilized in its HCl salt form, and its acidity predominantly originates from the protonation of the sulfonate group ( $-\text{SO}_3\text{H}$ ). All the tested DES were more polar than ethanol ( $\text{ENR} < 52.17 \text{ kcal mol}^{-1}$ ) and less polar (or of similar polarity) than water ( $\text{ENR} < 48.20 \text{ kcal mol}^{-1}$ ).<sup>48</sup> The measured densities of the DESs were in the range from 0.9 and  $1.2 \text{ g cm}^{-3}$ , with the majority falling in the  $1.1\text{--}1.2 \text{ g cm}^{-3}$  range at room temperature. Finally, we utilized FT-IR analysis for the chemical characterization of the prepared DESs, aiming to confirm the presence of strong interactions within the components. As anticipated, the FT-IR spectra of pure methylamines (betaine, TMAO and sarcosine) and amino acids (ectoine and proline) showed characteristic bands: the NH bond stretching ( $\nu(\text{NH})$ ) between  $3300\text{--}3500 \text{ cm}^{-1}$  and the carbonyl bond stretching ( $\nu(\text{C}=\text{O})$ ) between  $1600\text{--}1800 \text{ cm}^{-1}$  (Fig. S1–S2, ESI<sup>†</sup>). In the DESs spectra, we observed signals reminiscent of the starting materials, but with distinct features suggesting the formation of mixtures where hydrogen bonding predominates. Specifically, when methylamines or amino acids were paired with HBD (glycerol and urea) we noticed a broad, strong peak spanning from  $3650$  to  $3000 \text{ cm}^{-1}$ , indicating the formation of robust  $\text{NH}\cdots\text{O}=\text{C}$  hydrogen bonds between the components. Additionally, a shift towards higher wavenumbers in the carbonyl stretching ( $\nu(\text{C}=\text{O})$ ) band in the DESs spectra further supported the occurrence of hydrogen bonding.<sup>49</sup>

### The heat shock: quantitative monitoring of lysozyme colloidal and conformational stability in osmolyte-based DESs

**Heat induced aggregation and inactivation of lysozyme.** The propensity of novel osmolyte-based DESs to prevent aggregation of lysozyme during heat shock ( $80 \text{ }^\circ\text{C}$ ) was monitored by measuring the time-dependent optical density of the enzyme solution containing a relatively high concentration of the enzyme ( $5 \text{ mg ml}^{-1}$ ). Heat-induced aggregation of proteins above their melting point ( $\leq 70 \text{ }^\circ\text{C}$  for lysozyme, depending on the pH value),<sup>50</sup> accelerates the aggregation rate while mitigating complications associated with structural alterations. This phenomenon is frequently leveraged to investigate the

stabilizing effects of potential protein chaperones and understand the underlying principles guiding their mode of action.<sup>51</sup>

As can be seen in Fig. S3 (ESI<sup>†</sup>), in the reference buffer, a rapid increase in optical intensity signifies aggregation of the enzyme. Conversely, in DESs tested (including reference cholinium- and betaine-based DESs) no time-dependent aggregation of lysozyme was observed, except for TMAO:U (only data for buffer, TMAO:U, and a bioinspired multicomponent DES are shown). This chaperone-like activity of conventional cholinium-based DESs containing urea and polyols has already been observed for lysozyme<sup>18</sup> and immunoglobulin G.<sup>32</sup> Remarkably, even in DMSP:Gly with a pH value as low as 1.0, no aggregation was observed. This is noteworthy considering that, according to the literature, at temperatures of  $80 \text{ }^\circ\text{C}$  aggregation in lysozyme solutions typically initiates immediately at pH levels below 4.0.<sup>52</sup>

This simple and rapid aggregation test gave us valuable hints on osmolyte-based DESs' potential to act as chemical chaperones. Furthermore, the recovery of enzymatic activity after heat treatment was measured upon dilution in the buffer.<sup>34</sup> It is crucial to emphasize herein that in all bioactivity experiments, lysozyme solutions were incubated in DESs, and aliquots were subsequently withdrawn to measure the residual enzyme activity in the buffer.<sup>39</sup> This procedure was applied both at the initial time point ("zero"), where each enzyme solution in DES served as its own reference for subsequent activity measurements, and after treatments such as heat or cold shock. Thus, any potential effects of osmolytes on enzyme activity were minimized using this approach. Furthermore, enzyme activities measured immediately after dissolving lysozyme in DES (initial lysozyme activity in DES) were comparable to the initial activity of lysozyme in the reference sample. This suggests that the concentrations of osmolytes present during the enzyme activity measurements had no significant effect.

Fig. 1 shows the residual activity ( $A_R$ ) of lysozyme after the heat treatment. In the reference buffer,  $A_R$  decreased to approximately 20%, a value like the one observed for TMAO-based DESs. However, the remaining DESs exhibited greater enzyme stabilization. This effect was particularly notable in three DESs variants, all incorporating glycerol as the HBD: Bet:Gly, Sar:Gly, and Ect:Gly, where enzyme activity was fully preserved ( $A_R \geq 96\%$ ). Here, we have demonstrated that Sar:Gly ( $A_R = 120\%$ ), functioning as a DES with superior lysozyme stabilization ability, significantly surpasses ChCl:Gly ( $A_R = 78\%$ ), which has previously been indicated to stabilize lysozyme during thermal treatment at  $80 \text{ }^\circ\text{C}$ .<sup>44</sup> The observation that glycerol-based DESs function as excellent chemical chaperones aligns with previous studies by Delorme *et al.*<sup>25</sup> and Toledo *et al.*<sup>53</sup> that highlighted a positive relationship between higher counts of OH-groups in the HBD and improved thermostability through hydrogen bond formation between the OH-groups on the HBD and the enzyme's amino acids. In glycerol-based DESs the same authors also observed an increase in  $A_R$  values above 100%. To adequately explain this phenomenon, a more in-depth analysis is necessary. Although glycerol-based DESs herein demonstrated a higher stabilization ability compared to their urea-based counterparts, the latter still exhibited improved stabilization of



lysozyme compared to the reference system (except for TMAO-based DES).

Additionally, even though strongly acidic DES, specifically DMSP:Gly, demonstrated lower lysozyme stabilization potential compared to other glycerol-based DES, it unexpectedly exhibited a comparable stabilization ability to the reference buffer ( $A_R \sim 25\%$ ). This occurrence might be attributed to the abundance of HBA/HBD-acting groups, such as hydroxyl and carboxyl, which contribute to buffering the system through the formation of dense hydrogen bonds.<sup>54</sup> From the thermostability results, it appears that the pH value of a DES is not a critical factor in its ability to stabilize lysozyme. For example, despite having similar pH values, Sar:Gly, Sar:U and DMSP:U (ranging from 5.2 to 5.6), exhibited significantly different levels of lysozyme residual activity after heat shock (120%, 87%, and 40%, respectively). This observation is intriguing and suggests that other mechanisms may be at play, such as direct interactions between DES components and proteins, or interactions with water molecules in close proximity to the protein, thereby altering the water activity of the medium.

Finally, two bioinspired multicomponent DESs, both based on urea as an HBD, also showed excellent chaperon-like activity with  $A_R > 85\%$ . Similar to what was observed in our previous work,<sup>34</sup> two-component DESs consisting of betaine and TMAO with urea as the HBD demonstrated a lesser ability to stabilize lysozyme compared to their multicomponent bioinspired DES counterpart. This suggests once again that including additional osmolytes in the cocktail, in molar ratios replicated from a natural context, significantly enhances the DES's ability to stabilize lysozyme.

**Impact of individual and combined effects of the DES components on lysozyme stability.** To explore the individual and combined effects of DES components on enzyme stability, we analysed the distinct impacts of these components while keeping the water volume fraction constant at 40% (w/w)<sup>55</sup>

(Fig. 2A). As expected, we confirmed the synergistic behaviour of the betaine-urea mixture in stabilizing lysozyme.<sup>43</sup> After the heat shock, while the enzyme retained 10% and 43% of residual activity in urea or betaine solutions, respectively,  $A_R$  of 65% was observed in the Bet:U mixture. Similar trends were observed for sarcosine-, TMAO-, and proline-based DES, where urea served as the HBD: in terms of protein stabilization, these DESs (with  $A_R = 87\%$ , 18%, and 72%, respectively) not only attenuated the deleterious effect of urea but also outperformed water solutions of the corresponding individual HBA components ( $A_R = 75\%$ , 4%, and 48%, respectively). In ectoine- and DMSP-based DESs, the synergistic effect was less pronounced; however, both HBA components attenuated the deleterious effect of urea, resulting in enzyme stability superior to that in the reference buffer, with  $A_R > 40\%$ . It is noteworthy that the synergistic effects of the components were most pronounced in the two multicomponent bioinspired DESs: the addition of other components counteracted the deleterious effect of urea to a greater extent than corresponding binary mixtures, maintaining  $A_R > 85\%$ . Overall, the presented results reaffirm once again that kosmotropic osmolytes are effective in counterbalancing the deleterious effects of the kosmotrope urea, in a molar ratio close to 1:2.<sup>34</sup> It has been proposed that such kosmotrope counterbalancing is achieved through the attraction of urea molecules, preventing their interaction with the protein surface, or by hindering the mobility of urea molecules through hydrogen bonding with kosmotrope, thereby restricting their access to protein domains.<sup>56,57</sup>

In DESs where glycerol acted as the HBD, this kind of synergistic effect was only observed for Sar:Gly. Specifically, lysozyme retained its activity completely in the glycerol-water mixture ( $A_R \sim 100\%$ ), whereas in Sar:Gly, the enzyme was "overactivated" with an  $A_R = 120\%$ . However, in the other DESs, a cumulative effect was noted: all glycerol-based DESs exhibited superior enzyme stabilization capability compared to their HBA counterparts.

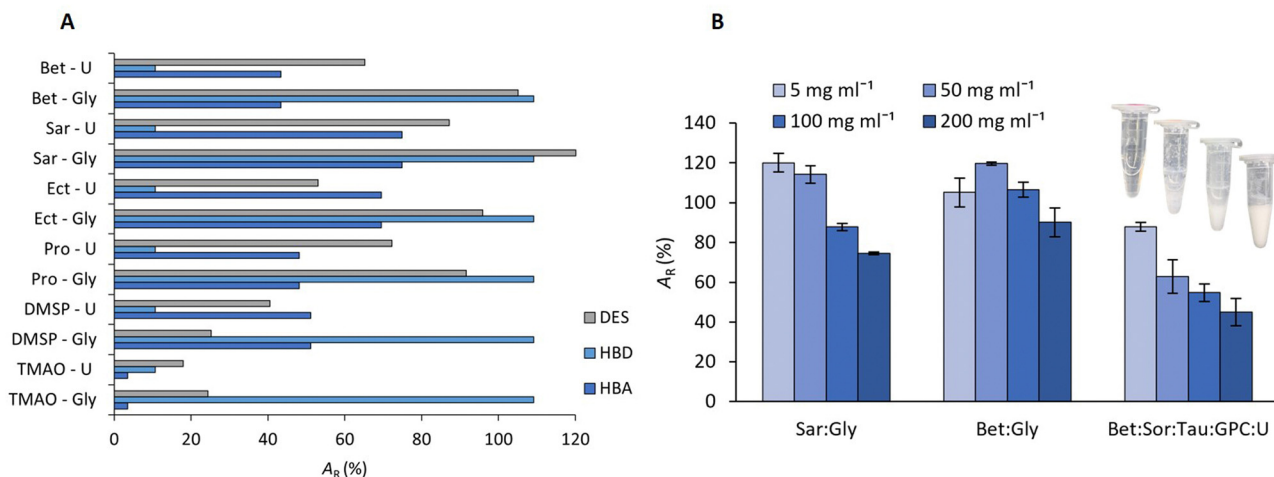


**Fig. 2** (A) Residual lysozyme activity ( $A_R$ ) after incubation in DESs and corresponding individual components (40% of water, w/w) after heat shock for 1 hour at 80 °C ( $c_{lys} = 5 \text{ mg ml}^{-1}$ ) and (B) residual lysozyme activity ( $A_R$ ) at different enzyme loadings (5, 50, 100 and 200  $\text{mg ml}^{-1}$ ) after incubation in DESs (40% of water, w/w) for 1 hour at 80 °C. The residual lysozyme activity ( $A_R$ ) was calculated from the initial reaction rate obtained by the enzyme after incubation, compared to the one obtained without previous exposure.



### Thermal stability of highly concentrated lysozyme solutions.

The current understanding of protein behaviour in DESs has primarily focused on extremely dilute conditions, neglecting their behaviour at concentrations relevant to technology ( $> 50 \text{ mg ml}^{-1}$ ). This knowledge gap hinders potential applications of DESs in protein stabilization, as storing or formulating proteins in such dilute conditions would demand impractical volumes of solvent.<sup>39</sup> Namely, the primary hurdle in formulating protein solutions at elevated concentrations lies in navigating the intricate degradation pathway driven by concentration-dependent aggregation.<sup>58</sup> To the best of our knowledge, the efficacy of DESs, specifically ChCl:Gly, in maintaining the physical integrity of lysozyme at high protein concentrations up to  $143 \text{ mg ml}^{-1}$  has been demonstrated only in the study by Sanchez-Fernandez *et al.*<sup>39</sup> Here, we evaluated the effectiveness of the three most promising DES candidates identified during the initial screening, Sar:Gly, Bet:Gly, and bioinspired multicomponent DES Bet:Sor:Tau:GPC:U, in stabilizing lysozyme across a broad concentration range, specifically from  $5$  to  $200 \text{ mg ml}^{-1}$ , while ensuring the protein remained soluble. As shown in Fig. 2B, in the bioinspired multicomponent DES there is a significant decrease in  $A_R$  value after heat shock, correlating with the enzyme loading ( $A_R = 45\%$  at a loading of  $200 \text{ mg ml}^{-1}$ ). Additionally, above a lysozyme concentration of  $5 \text{ mg ml}^{-1}$  protein aggregates were visibly formed in this DES after the heat shock. However, in Sar:Gly and Bet:Gly, lysozyme activity was fully preserved at loadings up to  $50 \text{ mg ml}^{-1}$ . At loadings of  $100$  and  $200 \text{ mg ml}^{-1}$ , a slight reduction in activity was observed in both DESs, but still with excellent recovery ( $A_R > 75\%$ ) and no observable aggregation.

**Near- and far-UV circular dichroism analysis of lysozyme solutions.** To validate the effectiveness of the several most promising osmolyte-based DES candidates in preventing the denaturation of lysozyme, the thermal unfolding of the protein was examined by monitoring changes in the enzyme's secondary and tertiary structure in both the far- and near-UV regions using circular dichroism (CD) spectroscopy.<sup>39,44,59–61</sup>

First, both buffered and DES solutions of lysozyme were monitored at a single wavelength in the far UV region. Upon heating, the negative CD signal intensity decreased. The melting curve displayed a sigmoidal shape, indicating a cooperative, two-state denaturation process for lysozyme in the buffered aqueous solution (Fig. 3). The transition temperature (thermal melting,  $T_m$ ), which signifies the temperature at which the protein undergoes structural transition or denaturation, resulting in the unfolding of its secondary and tertiary structure, was determined to be  $75.9 \text{ }^\circ\text{C}$ . A similar cooperative shape was observed for lysozyme solutions in DESs. All DESs tested (Bet:Gly, Sar:Gly, Pro:Gly, and bioinspired multicomponent DES Bet:Sor:Tau:GPC:U) exhibited a strong stabilizing influence on the protein's secondary structure. The  $T_m$  value of lysozyme in Pro:Gly exceeded that in the buffered aqueous solution by  $5 \text{ }^\circ\text{C}$ , and by more than  $10 \text{ }^\circ\text{C}$  in Bet:Gly, Sar:Gly, and Bet:Sor:Tau:GPC:U. The highest  $T_m$  value of  $91.5 \text{ }^\circ\text{C}$  was observed in Bet:Sor:Tau:GPC:U (Fig. S4 and Table S1, ESI<sup>†</sup>).

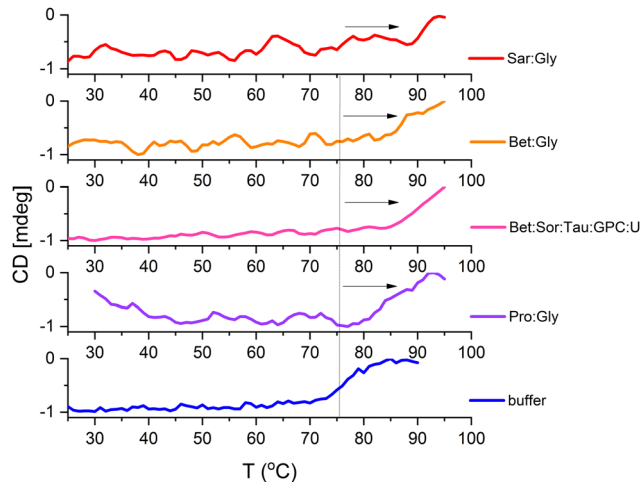


Fig. 3 Thermal CD scans of lysozyme in 50 mM potassium phosphate buffer (pH 6.4) and DESs containing 40% of water, w/w ( $c_{\text{Lys}} = 0.3\text{--}0.4 \text{ mg ml}^{-1}$ ;  $\lambda = 227 \pm 5 \text{ nm}$ ): ellipticity change is a consequence of secondary structure change.

While the far UV CD spectral region reflects changes in secondary structure, the near UV CD region ( $250\text{--}350 \text{ nm}$ ) serves as a fingerprint of the protein's tertiary structure. The near UV CD spectrum is influenced by aromatic amino acids and the rigidity of their surroundings, including intramolecular interactions such as hydrogen bonding.<sup>38</sup> Thus, following the CD research conducted by Esquembre *et al.*,<sup>44</sup> we recorded the near CD spectra of the enzyme's solutions during thermal treatment. This allowed us to determine whether renaturation of lysozyme after heat shock occurs in DESs upon cooling, or later upon dilution in buffer. At room temperature, the near CD spectra of lysozyme in the buffer and DES exhibited triplet-like signals attributed to tyrosine, tryptophan, and disulfide residues,<sup>38,62</sup> indicating a comparable tertiary structure of lysozyme in these solvents (Fig. 4 and Fig. S5, ESI<sup>†</sup>). The heating of the solution led to a featureless spectrum in all tested solutions, attributable to the unfolding of the protein and the exposure of the aromatic side chains of amino acids to the isotropic environment.<sup>41,43,44</sup> It is noteworthy that in DES solutions the tertiary structure was partially maintained even at  $80 \text{ }^\circ\text{C}$ , with complete protein unfolding occurring only at  $95 \text{ }^\circ\text{C}$ . Overall, CD studies confirmed that in osmolyte-based DESs with glycerol as the HBD and in multicomponent bioinspired DES lysozyme shows excellent thermostability and is able to entirely regain its folded structure after cooling to room temperature.

### The cold shock: quantitative monitoring of lysozyme stability in osmolyte-based DESs

To assess whether osmolyte-based DESs protect proteins during freeze–thaw cycles in a similar way, lysozyme solutions ( $5 \text{ mg ml}^{-1}$ ) underwent five consecutive cycles of freezing ( $-80 \text{ }^\circ\text{C}$  and  $-20 \text{ }^\circ\text{C}$ ) and thawing at room temperature. The residual enzyme activity ( $A_R$ ) was measured after each cycle, and the results are presented in Fig. 1 and Fig. S6 and S7 (ESI<sup>†</sup>).



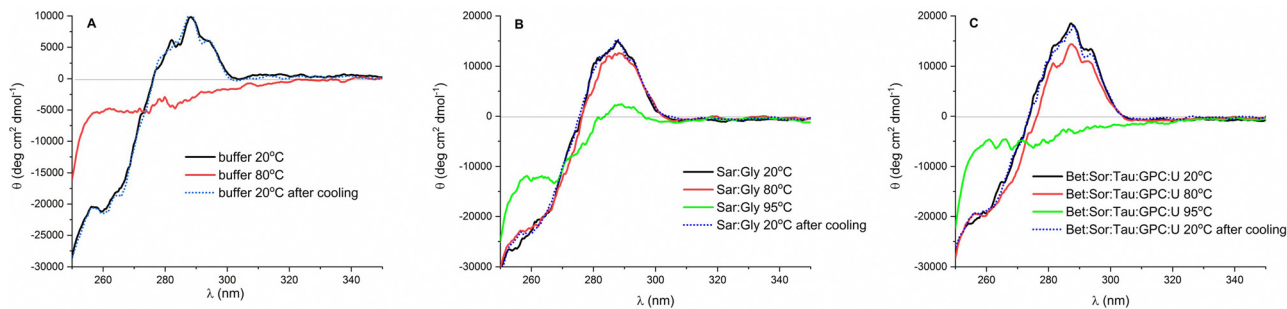


Fig. 4 Near UV CD spectra of lysozyme ( $c_{\text{Lys}} = 0.2 \text{ mg ml}^{-1}$ ) dissolved in (A) 50 mM potassium phosphate buffer (pH 6.4), (B) Sar:Gly (40% of water, w/w), and (C) Bet:Sor:Tau:GPC:U (40% of water, w/w) at 20 °C before thermal treatment (black line), at 80 °C (red line), 95 °C (green line) and at 20 °C after cooling (blue dotted line). CD spectra are normalized according to the CD spectra of lysozyme before thermal treatment.

Overall, a decrease in enzyme activity was observed in all DESs tested across consecutive freeze–thaw cycles at both storage temperatures, except for Sar:Gly and DMSP:U at  $-80$  °C, and DMSP:U at both temperatures. Notably, DMSP:U exhibited the best ability to stabilize lysozyme under cold shock, with  $A_{\text{R}} = 100\%$  after five freeze–thaw cycles at both storage temperatures. In comparison, lysozyme in the reference buffer exhibited a reduction in  $A_{\text{R}}$  to 45% and 75% at  $-80$  °C and  $-20$  °C, respectively. Moreover, osmolyte-based DESs again demonstrated chaperon-like activity superior to conventional choline chloride-based DESs. In heat-induced stress experiments, glycerol emerged as the most effective HBD among those tested. However, in scenarios involving cold-induced stress, DESs based on urea have proven to be equally effective candidates for enzyme stabilization as glycerol-based ones. The observation that DESs containing glycerol are effective in cryoprotecting proteins comes as no surprise, considering glycerol's well-established reputation as a protein cryoprotectant.<sup>63</sup> However, since urea has previously been demonstrated to promote enzyme inactivation during freeze–thawing,<sup>64</sup> this discovery is rather exciting. The results suggest that kosmotropes, such as sarcosine, ectoine, DMSP, and proline, effectively counteract the detrimental effects of urea on lysozyme during cold shock in deep eutectic environments: these mixtures provide more efficient protection for the enzyme compared to the reference buffer. On top of that, urea-based bioinspired multi-component DESs, especially TMAO:Bet:Tau:U, again showed excellent chaperon-like activity with  $A_{\text{R}} > 85\%$ , much higher than their two-component counterparts TMAO:U and Bet:U. This observation aligns well with natural phenomena: to reduce the cytoplasmic freezing point and fend off frost, psychrophilic bacteria, diapausing insects, amphibians, and reptiles accumulate urea, alongside other osmolytes such as betaine, sugars, sugar alcohols, and amino acids.<sup>34</sup>

#### Balancing enzyme activity and stability in DES–water mixtures: could transitions between dormant and active states of enzymes *in vivo* be explained through the formation of a DES?

The results presented in this study demonstrate: (i) the remarkable effectiveness of novel osmolyte-based DESs in stabilizing the model protein under stress conditions, and (ii) observable

changes in the protein structure during stress in DESs, which can nonetheless be fully restored upon returning the enzyme to ambient conditions. However, in line with prior findings,<sup>39,44</sup> we observed low or negligible enzyme activity in several of the most promising osmolyte-based DESs in terms of stabilization efficacy ( $<20\%$  compared to the activity measured in the reference buffer) (Fig. S8, ESI<sup>†</sup>) that could be completely recovered after dilution of the enzyme in the buffer (see the section ‘Heat induced aggregation and inactivation of lysozyme in DESs’).

Hence, we delved deeper into the intriguing relationship between enzyme activity and stability, focusing specifically on the bioinspired DES (Bet:Sor:Tau:GPC:U), and the dependence of these two enzyme's properties on water content (20, 40, 60 and 80% of water in DES, w/w). Again, lysozyme showed slight or no activity in the DES containing  $\leq 40\%$  of water (w/w), while the activity increased upon the addition of water, peaking in the highly diluted mixture (80% of water, w/w), however, the value was still much lower than that observed in the buffer (about 40% of the activity observed in the buffer) (Fig. 5). Conversely, enzyme stability (assessed by subjecting lysozyme to heat shock to elicit a rapid response), was notably better preserved in highly ‘‘concentrated’’ DES, reaching its peak at a water concentration of 20% (w/w) (Fig. 5). Temperature-dependent CD spectra of lysozyme solution in the DES in the temperature range 20–95 °C confirmed the results: the stabilization effect of DES with lower water content ( $\leq 40\%$ , w/w) is so strong that the full unfolding of the protein does not occur under the measurement conditions, as seen by the lack of a plateau in the melting curve (Fig. 6A and Fig. S9, ESI<sup>†</sup>). On the other hand, when approaching higher water concentrations, the unfolding of the enzyme follows a trend more similar to that in the buffer. Fig. 6B further highlights the observed dependence of lysozyme's transition temperatures on water content, showing a peak at 20% water in DES (w/w) with  $T_{\text{m}} = 93$  °C.

To investigate whether changes in the enzyme's behaviour in DES are associated with specific alterations in secondary structure, and whether these alterations can be reversed upon enzyme dilution in buffer, we initially recorded the far UV CD and FT-IR spectra of lysozyme in the ‘‘concentrated’’ Bet:Sor:Tau:GPC:U solution. Subsequently, we recorded the far UV CD



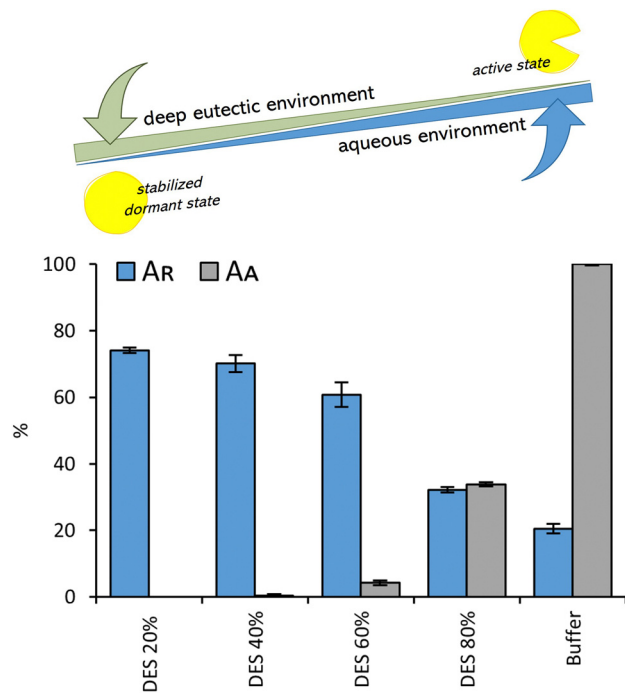


**Fig. 5** The interplay between the enzyme's active and stable (but inactive) states: residual lysozyme activity ( $A_R$ ) after heat shock (1 hour at 80 °C,  $c_{Lys} = 5 \text{ mg ml}^{-1}$ ) and relative lysozyme activity ( $A_A$ ) after incubation in DES (Bet: Sor: Tau: GPC: U) at different water shares (20, 40, 60 and 80%, w/w) and 50 mM potassium phosphate buffer (pH 6.4). The residual lysozyme activity ( $A_R$ ) was calculated from the initial reaction rate obtained by the enzyme after incubation, compared to the one obtained without previous exposure, while the relative enzyme activity ( $A_A$ ) was expressed as a ratio of activity measured in DES and activity measures in the reference buffer.

spectrum after diluting (rehydrating) lysozyme in buffer. Both the far UV CD and FT-IR spectra of the enzyme in the “concentrated” DES revealed noticeable peak wavelength shifts in

the Bet: Sor: Tau: GPC: U solution, indicating a greater presence of  $\beta$ -sheets (a structure more resistant to unfolding than  $\alpha$ -helices<sup>65,66</sup>) compared to lysozyme in its native state in buffer, where  $\alpha$ -helices predominate (Fig. 7A and B). Furthermore, the far UV spectra confirmed that upon rehydration of lysozyme preincubated in Bet: Sor: Tau: GPC: U into buffer, the native lysozyme secondary structure was virtually fully restored (Fig. 7A and Fig. S10, ESI†).

Overall, these findings suggest that the interplay between the enzyme's active and stable (but inactive) states is highly influenced by the water content in DES, supporting our hypothesis<sup>46</sup> that osmolyte mixtures form DES at the nano/microscale *in vivo*, preserving enzymes in a catalytically inactive state during stressful conditions such as cryoprotection, drought resistance, and germination, with the eutectic systems becoming diluted upon overcoming these stressors and the subsequent entry of water into the cell, leading to enzyme activation. Such readily reversible transitions between inactive and active enzyme states (dormancy and wake-up states) in response to alterations in its microenvironment (reactivation of lysozyme occurs within a minute following dilution from a “concentrated” DES, as observed during stability tests) would be energetically beneficial since metabolic regulation at the level of enzyme degradation or synthesis would be avoided.<sup>67</sup> Most importantly, the *in vivo* fluctuations of water content in the protein microenvironment and the resulting reversible interplay between active/dormant states would open a new window through which information flows in natural systems could be understood, investigated or even monitored.

Finally, it is crucial to acknowledge that the mechanisms by which protein structure is influenced by its environment are far more intricate than what is presented here, where only solvent-protein interactions are considered. *In vivo*, protein folding/unfolding occurs within the crowded cellular milieu, characterized by volume exclusion due to neighbouring soluble

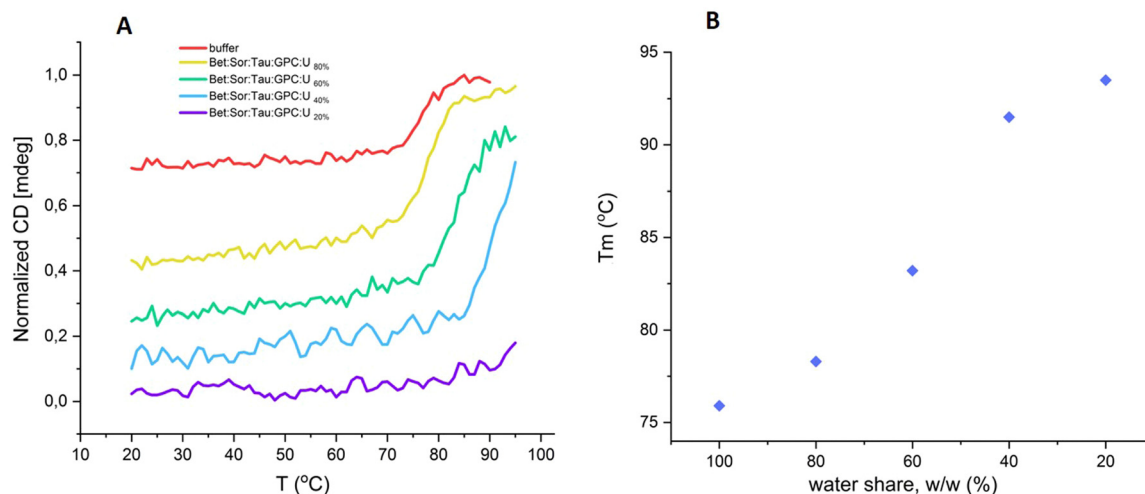


**Fig. 6** (A) Normalized ellipticity for lysozyme ( $c_{Lys} = 0.4 \text{ mg ml}^{-1}$ ;  $\lambda = 225 \text{ nm}$ ) in Bet: Sor: Tau: GPC: U at different water shares and 50 mM potassium phosphate buffer solution (pH 6.4) as a function of temperature; (B) relationship between the transition temperatures ( $T_m$ ) calculated for lysozyme and varying water content in a Bet: Sor: Tau: GPC: U (20, 40, 60 and 80%, w/w) ( $c_{Lys} = 0.4 \text{ mg ml}^{-1}$ ;  $\lambda = 225 \text{ nm}$ ).



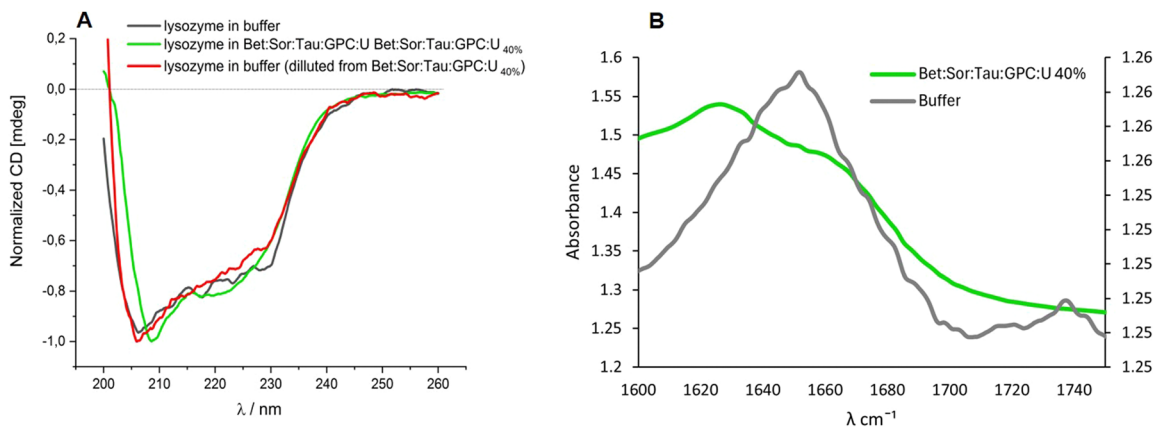


Fig. 7 (A) Far UV CD spectra of lysozyme dissolved in 50 mM potassium phosphate buffer (pH 6.4) ( $c_{\text{Lys}} = 0.2 \text{ mg ml}^{-1}$ ) and hydrated lysozyme (dilution of lysozyme solution pre-incubated in Bet: Sor: Tau: GPC: U (40% of water, w/w) into the buffer, resulting in a final concentration of Bet: Sor: Tau: GPC: U in the buffer of 0.5% (v/v) and (B) FTIR spectra of lysozyme ( $c_{\text{Lys}} = 0.2 \text{ mg ml}^{-1}$ ) at 25 °C dissolved in 50 mM potassium phosphate buffer (pH 6.4) and Bet: Sor: Tau: GPC: U (40% of water w/w).

macromolecules, and within confined spaces, influenced by rigid or fixed structures. These environments are distinctly different. Models of crowding examine the effects of varied concentrations of soluble crowding agents, such as polymers, while confinement models involve molecular meshes, pores, and channels, simulating cytoskeletal and extracellular matrix structures.<sup>68,69</sup> Given these considerations, it is reasonable to assume that proteins encounter more complex landscapes *in vivo* compared to those described here. These differences likely play a significant role in the protein folding and unfolding puzzle in DES environments and warrant further exploration. In the context of using DES for protein stabilization, an intriguing approach could involve designing solvent media that combine macromolecular crowders<sup>27</sup> or confining proteins into nanopores<sup>70</sup> with DES technology. This hybrid strategy could offer novel solutions for enhancing protein stability.

### Cytotoxicity assessment of osmolyte-based DESs

Finally, to assess DESs biocompatibility, the newly synthesized osmolyte-based DESs were tested at three different concentrations (100 mg ml<sup>-1</sup>, 500 mg ml<sup>-1</sup>, and 1000 mg ml<sup>-1</sup>) on three cell lines: Caco-2, HaCaT, and HeLa. These cell lines were selected to cover various potential applications of the tested DES, ranging from oral administration (intestinal, Caco-2), to topical (skin, HaCaT), to possible antiproliferative effects (tumor cell line, HeLa). This evaluation serves as a preliminary assessment of DES ecotoxicity as well as proof of their cytocompatibility with the used cells and whether they can proceed to further application. Because none of the tested DES caused 50% growth inhibition in any of the used cell lines, the EC<sub>50</sub> values were declared to be higher than 1000 mg L<sup>-1</sup> and DESs were considered to have low cytotoxicity and non-antiproliferative activity (EC<sub>50</sub> > 2000 mg L<sup>-1</sup> *i.e.*, > 5 mM) (Table 1). The only exception is DMPS: Gly, which significantly inhibited the growth of all three cell lines at concentrations of 500 mg ml<sup>-1</sup> and 1000 mg ml<sup>-1</sup>. This is probably due to the extremely low pH value of DMPS: Gly (1.0) which can denature

membrane proteins and cause cell death.<sup>71</sup> Despite the observed decrease in cell survival associated with DMPS: Gly, it is important to note that the tested concentrations ranging from 100 mg ml<sup>-1</sup> to 1000 mg ml<sup>-1</sup>, are exceptionally high. By testing these high concentrations, we took into account the estimation that cell lines are approximately ten times less sensitive than *in vivo* tests. Therefore, the overall conclusion is that the tested DESs pose no environmental hazards or risks to human health. However, additional investigations on other model organisms are certainly desirable for final confirmation of the safety of these newly synthesized solvents.

## Conclusion

In conclusion, our study demonstrates that DESs based on naturally occurring osmolytes, in all their variety, are excellent biocompatible chemical chaperones promoting the correct refolding of unfolded lysozyme *in vitro* after exposing the enzyme to stressful conditions, such as heat shock and repeated freezing–thawing cycles. Glycerol-based DESs with betaine, sarcosine, and ectoine as HBA stood out as the best candidates for stabilizing lysozyme under heat shock conditions, while the urea-based DES, specifically DMSP, provided the greatest stabilization of lysozyme under freezing conditions. Interestingly multicomponent bioinspired DESs (Bet: Sor: Tau: GPC: U and TMAO: Bet: Tau: U) were excellent stabilizing medium for lysozyme under both storage conditions, showing excellent chaperon-like activity, much higher than their two-component counterparts Bet: U and TMAO: U. Through an analysis of the intriguing relationship between enzyme activity and stability in DES, with a focus on a bioinspired DES (Bet: Sor: Tau: GPC: U) and the dependency of these enzyme properties on water content, we have demonstrated that highly concentrated DES efficiently stabilize lysozyme in its inactive form. Furthermore, lysozyme activation can be easily achieved by diluting the enzyme–DES mixture in water, supporting our hypothesis that the formation of DES *in vivo* could facilitate rapid and reversible transitions between inactive



(dormant) and active (wake-up) states in response to changes in their microenvironment. We propose that by mimicking the natural landscape of a specific protein through tracking osmolyte cocktails and replicating them *in vitro* through DES, it is feasible to engineer the ideal medium for this specific protein to be stored for a long term and resistant to fluctuations in storage temperature. The present study suggests that a template protein stability can be enhanced by carefully tailored DES, and that further experiments and careful optimization of DES formulations will be needed to elucidate working combinations for additional proteins beyond lysozyme. The ability to selectively tune a protein microenvironment has the potential to foster manufacturing sustainability “by design” across diverse industries.

The current study primarily focused on identifying and reporting the observed stabilization effects by screening a large number of DESs to showcase the concept of osmolyte-based DESs as excellent protein stabilizers against heat and freeze shock, rather than delving into the detailed mechanisms underlying these behaviors. Therefore, designing a comprehensive study that combines various experimental and computational techniques would provide detailed mechanistic insight into how osmolyte-based DESs stabilize proteins. This approach would help in understanding the specific interactions and environmental factors that contribute to protein stabilization, thereby guiding the development of more effective DES formulations for biotechnological applications. Addressing this aspect is a key goal for our future research endeavors.

## Author contributions

The concept for the article was jointly conceived and developed by M. C. B. and T. A., while M. C. B. designed the experiments, wrote the first draft and provided direction. I. R. R. and L. T. helped refine the concept. M. C. B., L. T., A. D. and M. L. performed the experiments. The paper was reviewed and edited by all authors.

## Data availability

The data supporting this article have been included as part of the ESI.†

## Conflicts of interest

There are no conflicts to declare.

## Acknowledgements

This work was supported by the Croatian Science Foundation (IPS-2022-02-3938, IP-2019-04-7712 and IP-2018-01-4694). We gratefully acknowledge undergraduate students Marija Karin and Petra Lacić for their contributions to the experiments.

## Notes and references

- 1 V. A. Borzova, T. B. Eronina, V. V. Mikhaylova, S. G. Roman, A. M. Chernikov and N. A. Chebotareva, *Int. J. Mol. Sci.*, 2023, **24**, 10298.
- 2 R. J. Falconer, *Biotechnol. Adv.*, 2019, **37**, 107412.
- 3 M. C. Rodríguez, J. Villarraza, M. B. Tardivo, S. Antuña, D. Fontana, N. Ceaglio and C. Prieto, *J. Pharm. Sci.*, 2023, **112**, 2756–2765.
- 4 M. M. C. H. van Schie, J. D. Spöring, M. Bocola, P. Domínguez de María and D. Rother, *Green Chem.*, 2021, **23**, 3191–3206.
- 5 M. Akbarian and S.-H. Chen, *Pharmaceutics*, 2022, **14**, 2533.
- 6 S. R. Wlodarczyk, D. Custódio, A. Pessoa and G. Monteiro, *Eur. J. Pharm. Biopharm.*, 2018, **131**, 92–98.
- 7 L. Zhang, R. Zhou, J. Zhang and P. Zhou, *Int. Dairy J.*, 2021, **123**, 105175.
- 8 J. W. Bye, L. Platts and R. J. Falconer, *Biotechnol. Lett.*, 2014, **36**, 869–875.
- 9 G. Lentzen and T. Schwarz, *Appl. Microbiol. Biotechnol.*, 2006, **72**, 623–634.
- 10 T. Ueda, M. Nagata and T. Imoto, *J. Biochem.*, 2001, **130**, 491–496.
- 11 S. Khan, S. Siraj, M. Shahid, M. M. Haque and A. Islam, *Int. J. Biol. Macromol.*, 2023, **234**, 123662.
- 12 P. H. Yancey, *J. Exp. Biol.*, 2005, **208**, 2819–2830.
- 13 N. Zhang, P. Domínguez de María and S. Kara, *Catalysts*, 2024, **14**, 84.
- 14 A. M. Curreri, S. Mitragotri and E. E. L. Tanner, *Adv. Sci.*, 2021, **8**, 2004819.
- 15 A. P. Abbott, G. Capper, D. L. Davies, R. K. Rasheed and V. Tambyrajah, *Chem. Commun.*, 2003, 70–71.
- 16 Y. Zhou, W. Xu, Y. Pan, F. Wang, X. Hu, Y. Lu and M. Jiang, *BioResources*, 2022, **17**, 5485–5509.
- 17 D. O. Abranches and J. A. P. Coutinho, *Annu. Rev. Chem. Biomol. Eng.*, 2023, **14**, 141–163.
- 18 F. Niknaddaf, S. S. Shahangian, A. Heydari, S. Hosseinkhani and R. H. Sajedi, *ChemistrySelect*, 2018, **3**, 10603–10607.
- 19 P. Xu, Y. Wang, J. Chen, X. Wei, W. Xu, R. Ni, J. Meng and Y. Zhou, *Talanta*, 2019, **202**, 1–10.
- 20 Z. Takaloo, F. Niknaddaf, S. S. Shahangian, A. Heydari, S. Hosseinkhani and R. H. Sajedi, *Biotechnol. Appl. Biochem.*, 2020, **67**, 330–342.
- 21 S. H. Kim, S. Park, H. Yu, J. H. Kim, H. J. Kim, Y. H. Yang, Y. H. Kim, K. J. Kim, E. Kan and S. H. Lee, *J. Mol. Catal. B Enzym.*, 2016, **128**, 65–72.
- 22 I. Juneidi, M. Hayyan, M. A. Hashim and A. Hayyan, *Biochem. Eng. J.*, 2017, **117**, 129–138.
- 23 M. Shehata, A. Unlu, U. Sezerman and E. Timucin, *J. Phys. Chem. B*, 2020, **124**, 8801–8810.
- 24 N. Yadav, K. Bhakuni, M. Bisht, I. Bahadur and P. Venkatesu, *ACS Sustainable Chem. Eng.*, 2020, **8**, 10151–10160.
- 25 A. E. Delorme, J. M. Andanson and V. Verney, *Int. J. Biol. Macromol.*, 2020, **163**, 919–926.
- 26 H. Sun, R. Xin, D. Qu and F. Yao, *J. Biotechnol.*, 2020, **323**, 264–273.



- 27 K. Bhakuni, N. Yadav and P. Venkatesu, *Phys. Chem. Chem. Phys.*, 2020, **22**, 24410–24422.
- 28 B. P. Wu, Q. Wen, H. Xu and Z. Yang, *J. Mol. Catal. B: Enzym.*, 2014, **101**, 101–107.
- 29 A. A. N. Gunny, D. Arbain, E. M. Nashef and P. Jamal, *Bioresour. Technol.*, 2015, **181**, 297–302.
- 30 M. S. Lee, K. Lee, M. W. Nam, K. M. Jeong, J. E. Lee, N. W. Kim, Y. Yin, S. Y. Lim, D. E. Yoo, J. Lee and J. H. Jeong, *J. Ind. Eng. Chem.*, 2018, **65**, 343–348.
- 31 J. Hoppe, R. Drozd, E. Byzia and M. Smiglak, *Int. J. Biol. Macromol.*, 2019, **136**, 296–304.
- 32 D. Dhiman, A. S. C. Marques, M. Bisht, A. P. M. Tavares, M. G. Freire and P. Venkatesu, *Green Chem.*, 2023, **25**, 650–660.
- 33 I. Gomes and N. Galamba, *J. Chem. Phys.*, 2023, **159**, 235101.
- 34 M. Cvjetko Bubalo, T. Andreou, M. Panić, M. Radović, K. Radošević and I. R. Redovniković, *Green Chem.*, 2023, **25**, 3398–3417.
- 35 K. M. Jeong, J. Ko, J. Zhao, Y. Jin, D. E. Yoo, S. Y. Han and J. Lee, *J. Cleaner Prod.*, 2017, **151**, 87–95.
- 36 D. Shugar, *Biochim. Biophys. Acta*, 1952, **8**, 302–309.
- 37 P. Angsantikul, K. Peng, A. M. Curreri, Y. Chua, K. Z. Chen, J. Ehondor and S. Mitragotri, *Adv. Funct. Mater.*, 2021, **31**, 2002912.
- 38 S. M. Kelly, T. J. Jess and N. C. Price, *Biochim. Biophys. Acta, Proteins Proteomics*, 2005, **1751**, 119–139.
- 39 A. Sanchez-Fernandez, S. Prevost and M. Wahlgren, *Green Chem.*, 2022, **24**, 4437–4442.
- 40 R. Swaminathan, V. K. Ravi, S. Kumar, M. V. S. Kumar and N. Chandra, *Adv. Protein Chem. Struct. Biol.*, 2011, **84**, 63–111.
- 41 A. Sanchez-Fernandez, K. J. Edler, T. Arnold, D. Alba Venero and A. J. Jackson, *Phys. Chem. Chem. Phys.*, 2017, **19**, 8667–8670.
- 42 K. Park, B. Y. Ham, K. Li, S. Kang, D. Jung, H. Kim, Y. Liu, I. Hwang and J. Lee, *J. Mol. Liq.*, 2022, **349**, 118143.
- 43 C. X. Zeng, S. J. Qi, R. P. Xin, B. Yang and Y. H. Wang, *J. Mol. Liq.*, 2016, **219**, 74–78.
- 44 R. Esquembre, J. M. Sanz, J. G. Wall, F. Del Monte, C. R. Mateo and M. L. Ferrer, *Phys. Chem. Chem. Phys.*, 2013, **15**, 11248–11256.
- 45 A. Mitar, M. Panić, J. Prlić Kardum, J. Halambek, A. Sander, K. Zagajski Kučan, I. Radojčić Redovniković and K. Radošević, *Chem. Biochem. Eng. Q.*, 2019, **33**, 1–18.
- 46 D. Rente, M. Cvjetko Bubalo, M. Panić, A. Paiva, B. Caprin, I. Radojčić Redovniković and A. R. C. Duarte, *J. Cleaner Prod.*, 2022, **380**, 135147.
- 47 L. Cicco, G. Dilauro, F. M. Perna, P. Vitale and V. Capriati, *Org. Biomol. Chem.*, 2021, **19**, 2558–2577.
- 48 M. A. Karadendrou, I. Kostopoulou, V. Kakokefalou, A. Tzani and A. Detsi, *Catalysts*, 2022, **12**, 249.
- 49 B. Ozturk, C. Parkinson and M. Gonzalez-Miquel, *Sep. Purif. Technol.*, 2018, **206**, 1–13.
- 50 M. Hirai, S. Arai, H. Iwase and T. Takizawa, *J. Phys. Chem. B*, 1998, **102**, 1308–1313.
- 51 D. Shah, A. R. Shaikh, X. Peng and R. Rajagopalan, *Biotechnol. Prog.*, 2011, **27**, 513–520.
- 52 L. N. Arnaudov and R. De Vries, *Biophys. J.*, 2005, **88**, 515.
- 53 M. L. Toledo, M. M. Pereira, M. G. Freire, J. P. A. Silva, J. A. P. Coutinho and A. P. M. Tavares, *ACS Sustainable Chem. Eng.*, 2019, **7**, 11806–11814.
- 54 A. Salvi, J. M. Quillan and W. Sadee, *AAPS PharmSci*, 2002, **4**, 1–8.
- 55 J. P. Bittner, N. Zhang, L. Huang, P. Domínguez De María, S. Jakobtorweihen and S. Kara, *Green Chem.*, 2022, **24**, 1120–1131.
- 56 H. Monhemi, M. R. Housaindokht, A. A. Moosavi-Movahedi and M. R. Bozorgmehr, *Phys. Chem. Chem. Phys.*, 2014, **16**, 14882–14893.
- 57 S. Sarkar, S. Ghosh and R. Chakrabarti, *RSC Adv.*, 2017, **7**, 52888–52906.
- 58 S. J. Shire, Z. Shahrokh and J. Liu, *J. Pharm. Sci.*, 2004, **93**, 1390–1402.
- 59 L. Z. Wu, B. L. Ma, Y. B. Sheng and W. Wang, *J. Mol. Struct.*, 2008, **891**, 167–172.
- 60 T. Knubovets, J. J. Osterhout, P. J. Connolly and A. M. Klibanov, *Proc. Natl. Acad. Sci. U. S. A.*, 1999, **96**, 1262–1267.
- 61 A. Esposito, L. Comez, S. Cinelli, F. Scarponi and G. Onori, *J. Phys. Chem. B*, 2009, **113**, 16420–16424.
- 62 F. Tanaka, L. S. Forster, P. K. Pal and J. A. Rupley, *J. Biol. Chem.*, 1975, **250**, 6977–6982.
- 63 S. K. Singh and S. Nema, in *Formulation and Process Development Strategies for Manufacturing Biopharmaceuticals*, ed. F. Jameel and S. Hershenson, John Wiley & Sons, New Jersey, 2010, vol. 26, pp. 625–675.
- 64 J. F. Carpenter and J. H. Crowe, *Cryobiology*, 1988, **25**, 244–255.
- 65 R. Arunkumar, C. J. Drummond and T. L. Greaves, *Front. Chem.*, 2019, **7**, 74.
- 66 D. E. Otzen, *Biophys. J.*, 2002, **83**, 2219–2230.
- 67 P. H. Yancey, M. E. Clark, S. C. Hand, R. D. Bowlus and G. N. Somero, *Science*, 1982, **217**, 1214–1222.
- 68 D. Lucent, V. Vishal and V. S. Pande, *Proc. Natl. Acad. Sci. U. S. A.*, 2007, **104**, 10430–10434.
- 69 L. W. Simpson, T. A. Good and J. B. Leach, *Biotechnol. Adv.*, 2020, **42**, 107573.
- 70 D. L. Z. Caetano, R. Metzler, A. G. Cherstvy and S. J. de Carvalho, *Phys. Chem. Chem. Phys.*, 2021, **23**, 27195–27206.
- 71 L. Lomba, M. P. Ribate, E. Zaragoza, J. Concha, M. P. Garralaga, D. Errazquin, C. B. García and B. Giner, *Appl. Sci.*, 2021, **11**, 10061.

